BRL

REPORT
NO. 1279

AD

BRL R 1279

DYNAMICS OF LIQUID-FILLED SHELL: RESONANCE AND EFFECT OF VISCOSITY

By B. G. Karpov

MAY 1965

U. S. ARMY MATERIEL COMMAND
BALLISTIC RESEARCH LABORATORIES
ABERDEEN PROVING GROUND, MARYLAND

PAGES _____

ARE

MISSING

IN

ORIGINAL

DOCUMENT

SECURITY MARKING

The classified or limited status of this report applies to each page, unless otherwise marked.
Separate page printouts MUST be marked accordingly.

THIS DOCUMENT CONTAINS INFORMATION AFFECTING THE NATIONAL DEFENSE OF THE UNITED STATES WITHIN THE MEANING OF THE ESPIONAGE LAWS, TITLE 18, U.S.C., SECTIONS 793 AND 794. THE TRANSMISSION OR THE REVELATION OF ITS CONTENTS IN ANY MANNER TO AN UNAUTHORIZED PERSON IS PROHIBITED BY LAW.

NOTICE: When government or other drawings, specifications or other data are used for any purpose other than in connection with a definitely related government procurement operation, the U. S. Government thereby incurs no responsibility, nor any obligation whatsoever; and the fact that the Government may have formulated, furnished, or in any way supplied the said drawings, specifications, or other data is not to be regarded by implication or otherwise as in any manner licensing the holder or any other person or corporation, or conveying any rights or permission to manufacture, use or sell any patented invention that may in any way be related thereto.

Destroy this report when it is no longer needed.
Do not return it to the originator.

DDC AVAILABILITY NOTICE

Qualified requesters may obtain copies of this report from DDC.

Release or announcement to the public is not authorized.

The findings in this report are not to be construed as an official Department of the Army position, unless so designated by other authorized documents.

B A L L I S T I C R E S E A R C H L A B O R A T O R I E S

REPORT NO. 1279

MAY 1965

DYNAMICS OF LIQUID-FILLED SHELL: RESONANCE AND EFFECT OF VISCOSITY

B. G. Karpov

Exterior Ballistics Laboratory

RDT & E Project No. 1M010501A009

A B E R D E E N P R O V I N G G R O U N D , M A R Y L A N D

B A L L I S T I C R E S E A R C H L A B O R A T O R I E S

REPORT NO. 1279

BGKarpov/blw
Aberdeen Proving Ground, Md.
May 1965

DYNAMICS OF LIQUID-FILLED SHELL: RESONANCE AND EFFECT OF VISCOSITY

ABSTRACT

Experiments have been conducted with liquid-filled shell in free flight and with a liquid-filled gyroscope. The cavities in each were designed to have a principal fluid frequency which was equal to the nutational frequency of the respective systems.

Comparison of experimental results with predictions of the inviscid theory of Stewartson showed significant Reynolds number effects. Both the rate of divergence of the nutational amplitude at resonance and the width of the resonarce band are Reynolds number dependent. Also, there is a small shift of resonance frequency with Reynolds number. The experiments suggest, however, that in the limit, for large Reynolds numbers of the order of 10^6, the inviscid theory gives excellent predictions.

TABLE OF CONTENTS

1. INTRODUCTION

Earlier experiments in the free flight range[1*] have provided data on the dynamic behavior of liquid-filled shell during the very early part of their trajectory. Observation showed that during spin-up of the liquid, the shell were dynamically unstable for all fill conditions of practical interest. Moreover, the instability, or the rate of divergence of the nutational component of yaw, depended markedly on the specific gravity of the liquid; i.e., for heavier liquids the divergence of yaw was more rapid. For example, mercury-filled shell developed more than 80° of yaw in 150 feet of travel from the muzzle. It was also found that the spin-up of the liquid, as measured by the loss of angular momentum of the shell in vacuum, was markedly accelerated by the development of secondary flow within the cavity due to end effects. A theory for this phenomenon has been developed and is in good agreement with the experiments[2].

In the above experiments, no specific attempt was made to verify Stewartson's theory[3] because for the particular cavity used, the predicted resonance occurred only at 45 percent fill-ratio and relatively few firings were done at this loading.

To the best of our knowledge, Stewartson's theory has been previously tested only twice. The first experiments were done by firing, at long ranges, specially modified shell some of which were deliberately designed to be unstable (resonate) according to Stewartson's criteria, and others to be stable. These experiments were spectacularly successful. The second experiments were made by G. N. Ward[3] with a gyrostat. Ward found good agreement with the theoretical prediction of the fill-ratio at which the principal mode of instability should occur. However, he also found that the resonance band, or the range of fill-ratio over which the gyrostat was unstable, was more than twice as broad as theoretically predicted. Considerations of various sources which might have contributed to this discrepancy led to inconclusive results.

---

* *Superscript numbers denote references found on page* 39.

In view of the importance which Stewartson's theory may be expected to play in the design of liquid-filled shell, it appeared desirable to examine this discrepancy further. Therefore, free flight tests were conducted in the inclosed range under carefully controlled experimental conditions. These tests were supplemented by tests with a liquid-filled gyroscope. The gyroscope permitted tests over a wide range of Reynolds numbers.

This report describes the results of these experiments.

2. FREE FLIGHT FIRINGS

The shell for these experiments were 20mm models. A schematic drawing of the model is shown in Figure 1. The models were machined from solid aluminum bar stock to have cylindrical cavities of prescribed fineness ratios. The cavities were designed so that one of the principal frequencies of the fluid was close to the nutational frequency of the shell. The aerodynamic characteristics of this configuration were well known from previous work[4]. These and other characteristics as inferred from the present firings are discussed in Appendix 1.

To test Stewartson's theory, the fluid must be fully spinning. Consequently, with inclosed range firings the fluid must come to full spin very rapidly. Previous tests showed that glycerine, $\nu = 1000$ centistokes, reaches full spin in about 40 feet of travel from the muzzle. The remaining 240 feet of the range could then be used for relevant observations during which the shell executes about ten nutational oscillations. From prior physical and aerodynamic measurements the non-dimensional nutational frequency of the model, τ_n, was estimated to be 0.06. The cavity was to be filled to 90 percent ($b^2/a^2 = .10$). Therefore, from Stewartson's tables[3,5], any cavity with height 2c and diameter 2a or fineness ratio

$$c/a = 1.051\ (2j + 1) \qquad j = 0, 1, 2, \ldots.$$

will have as its principal fluid frequency τ_o equal to the nutational frequency of the shell $\tau_n = .06$. For $j = 1$, $c/a = 3.153$.

20 mm MODEL : 5 CAL. AN. SPINNER ROCKET

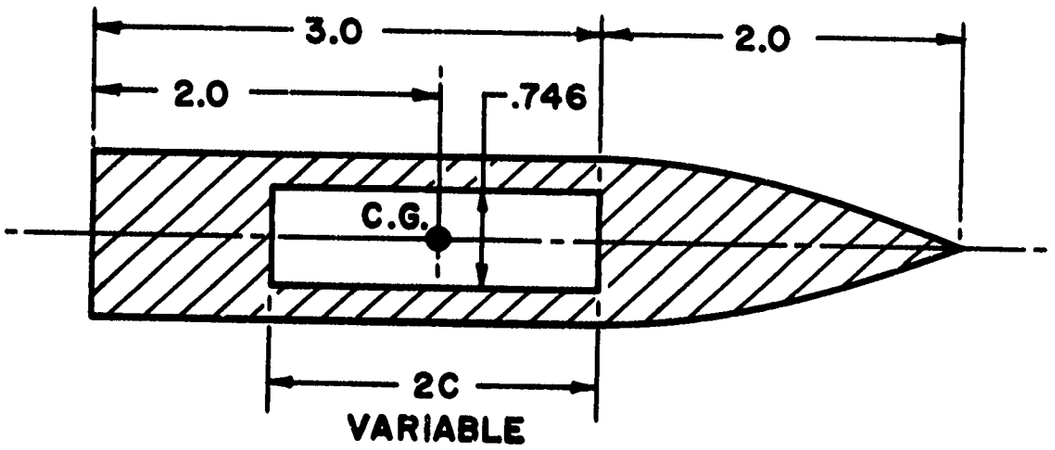

ALL DIMENSIONS ARE IN CALIBERS

FIGURE 1

In order to cover a broader range of fluid frequencies, it was decided to set the fill-ratio at 90 percent and vary the fineness ratio from 3.03 to 3.29. This variation of c/a permits testing of shell response to fluid frequencies varying from $\tau_o = .03$ to $\tau_o = .09$. At a constant fineness ratio, say c/a = 3.153, by varying fill-ratio, the lowest attainable frequency at 100 percent fill would have been $\tau_o = .047$ producing an asymmetrical distribution about $\tau_n = .06$.

The observed nutational yaw damping rates of the liquid-filled models, corrected for normal aerodynamic damping, are shown in Figure 2. These were obtained by the usual analysis of range firings. Also shown are theoretically predicted rates. As can be seen, there are significant differences between the theoretically predicted and the observed behaviors. We shall defer discussion of these differences until after presentation of the experimental results from the gyroscope tests.

3. GYROSCOPE

3.1 Description of the Apparatus:

The instrument shown in Plate 1 was originally designed and built during the last war to study the dynamics of liquid-filled shell. The rotor was a modified 4" shell which was driven by an air turbine, the air being admitted through the outer and inner gimbals.

For our purpose it was altered by discarding certain components. A new rotor was built containing a removable lucite cylindrical cavity of maximum inner diameter 2.50" and height 12.90" or fineness ratio c/a = 5.16. The full capacity of this cavity is 1038 cc. Unfortunately the center of the cavity was above the pivot point which presented certain experimental inconvenience. However, the center of mass of the whole system could be varied by adjustable rings on the rotor and the inner gimbal. Most of the experiments were conducted with the gyroscope in a stable position; i.e., with the center of mass of the system below the pivot point. The inner and outer gimbals were mounted on ball bearings.

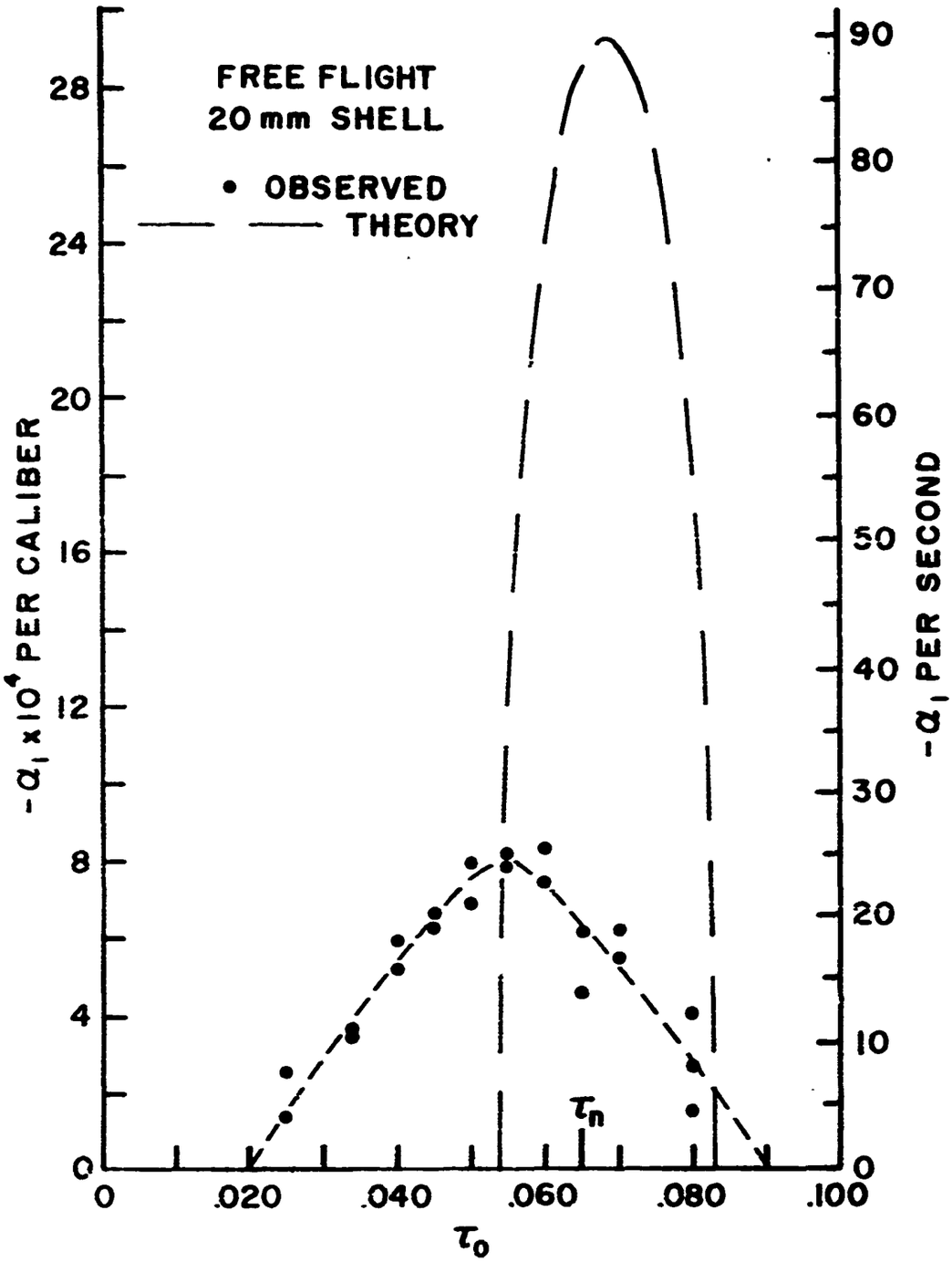

OBSERVED NUTATIONAL YAW DAMPING RATES OF LIQUID-FILLED MODELS

FIG. 2

The oscillations, about one gimbal axis, were measured with strain gages mounted on a strip of .015" stainless steel shim stock. The strip was spring loaded and attached to the outer gimbal, see Plate 1. The gages formed part of a bridge circuit whose amplified output was monitored on a photographic recorder. Two records are shown in Figure 3.

The spin of the rotor was measured by a small pick-up coil mounted on the inner gimbal and two small magnets on the rotor. The output was recorded on a tachometer and on an electronic counter. The rotor could be spun in excess of 10,000 rpm with reasonable safety; however, most of the experiments were conducted at lower spins.

The transverse moment of inertia of the gyroscope could be varied, within narrow limits, by the adjustable rings. An example of the characteristics of the gyroscope with empty cavity (c/a = 5.16) and certain position of the rings is:

Weight, rotor and inner gimbal, lbs.		25.80
Moments of inertia:	I_{x_o}, lbs-in^2	32.52
	I_{y_o}, lbs-in^2	865.5
	I_{z_o}, lbs-in^2	833.8
	$I \equiv \sqrt{I_{y_o} I_{z_o}}$	850

$$\therefore \quad \tau_n \doteq \frac{I_{x_o}}{I} = .038$$

3.2 Experimental Results:

From preliminary experiments with a completely filled (c/a = 5.16) cavity, the nutational frequency of the gyroscope was found to be closer to .040 than to .038 as given above. For this cavity, from Stewartson's tables, one finds that resonance, i.e., $\tau_o = \tau_n = .040$, should occur at 92 percent fill-ratio. The resonance, at this fill-ratio, should occur in any cavity whose fineness ratio satisfies the condition

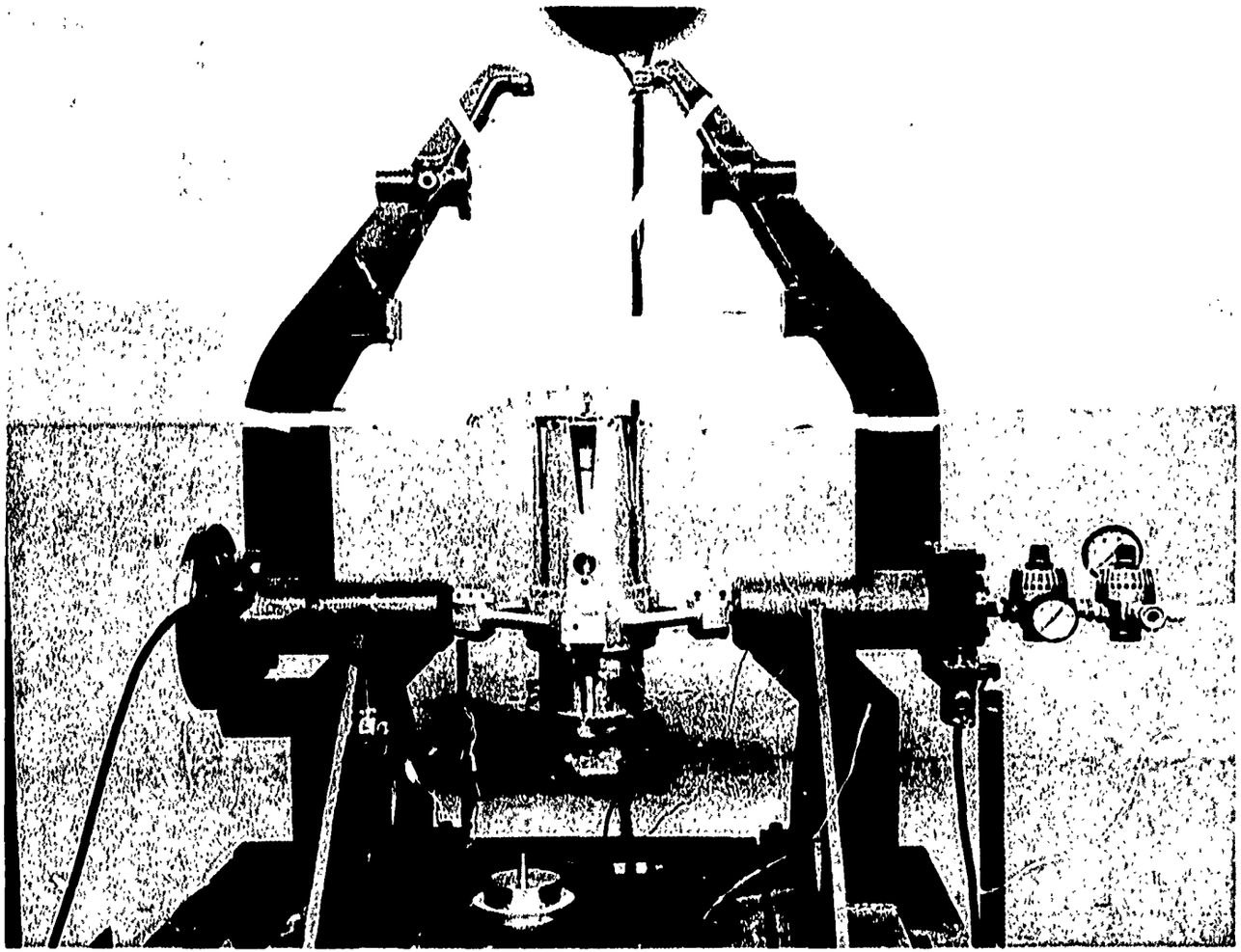

PLATE 1

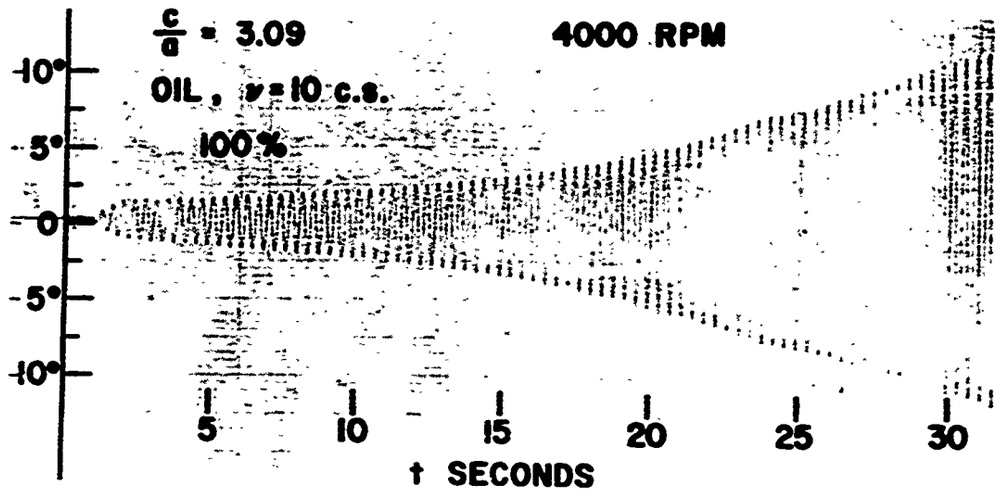
c/a = 3.09
4000 RPM
OIL, ν = 10 c.s.
100 %
10°
5°
0
-5°
-10°
5
10
15
20
25
30
t SECONDS

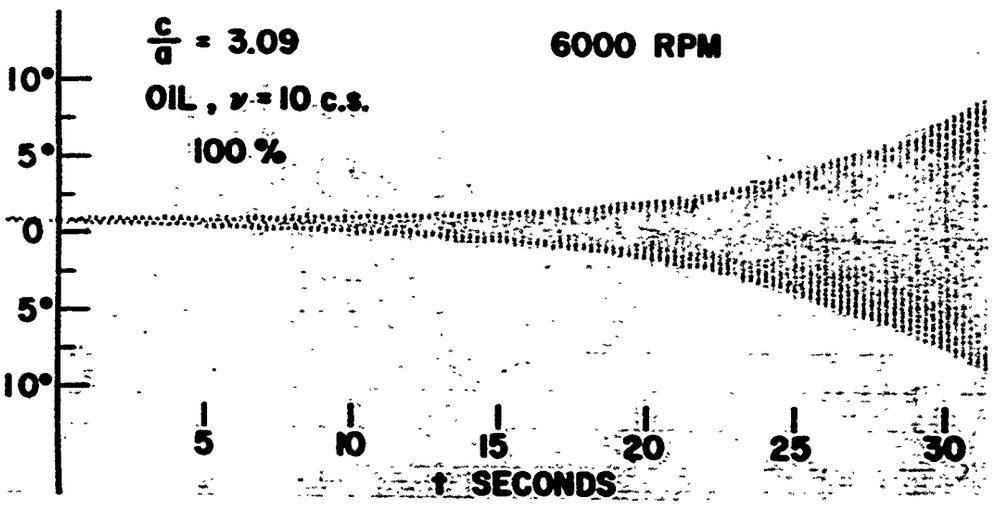
c/a = 3.09
6000 RPM
OIL, ν = 10 c.s.
100 %
10°
5°
0
5°
10°
5
10
15
20
25
30
t SECONDS

FIG. 3

$$c/a = 1.032\ (2j + 1) \qquad j = 0, 1, 2....$$

Thus, for $j = 1$, $c/a = 3.10$; for $j = 2$, $c/a = 5.16$, etc. Both of these cavities were used.

In order to cover a broad range of Reynolds numbers, the following liquids were tested:

Liquid	ρ, gm/cc	ν, c.s.
Mercury	13.6	0.1
Water	1	1
Silicon Oil	1	10
Glycerine	1.25	1000

Preliminary to various tests with liquids, runs were made with empty gyroscope in order to establish the nutational damping rate due to bearing friction. The damping was always small, about .017 per second, and was applied as a correction in all tests.

A characteristic of the tests with liquids was that instability was self-generating only in the vicinity of resonance. The width of the resonance band within which self-generation occurs (either in terms of ± percent of fill, or $\pm\tau_o$'s) increased with higher spin, higher specific gravity of the liquid, and lower j values. The effect of spin can be seen in Figure 3. For $c/a = 3.09$ and 100 percent fill, the instability is self-generating at 6000 rpm; at 4000 rpm an artificial initial disturbance was necessary.

For the $c/a = 5.16$ cavity, the combined experimental results and theoretical prediction are shown in Figure 4. Figure 5 shows the results for oil and glycerine at 4000 and 6000 rpm in greater detail. Similarly, Figures 6 and 7 show the experimental results for $c/a = 3.09$.

As can be seen from Figures 4 through 7, the resonance band at shorter frequencies, i.e., higher fill-ratios, is cut-off at about $\tau_o = 0.30$, producing a truncated distribution. To test whether the resonance band is symmetrical about its maximum, a slightly shorter cavity, $c/a = 3.03$, was tested. Shortening the cavity has the effect of shifting the

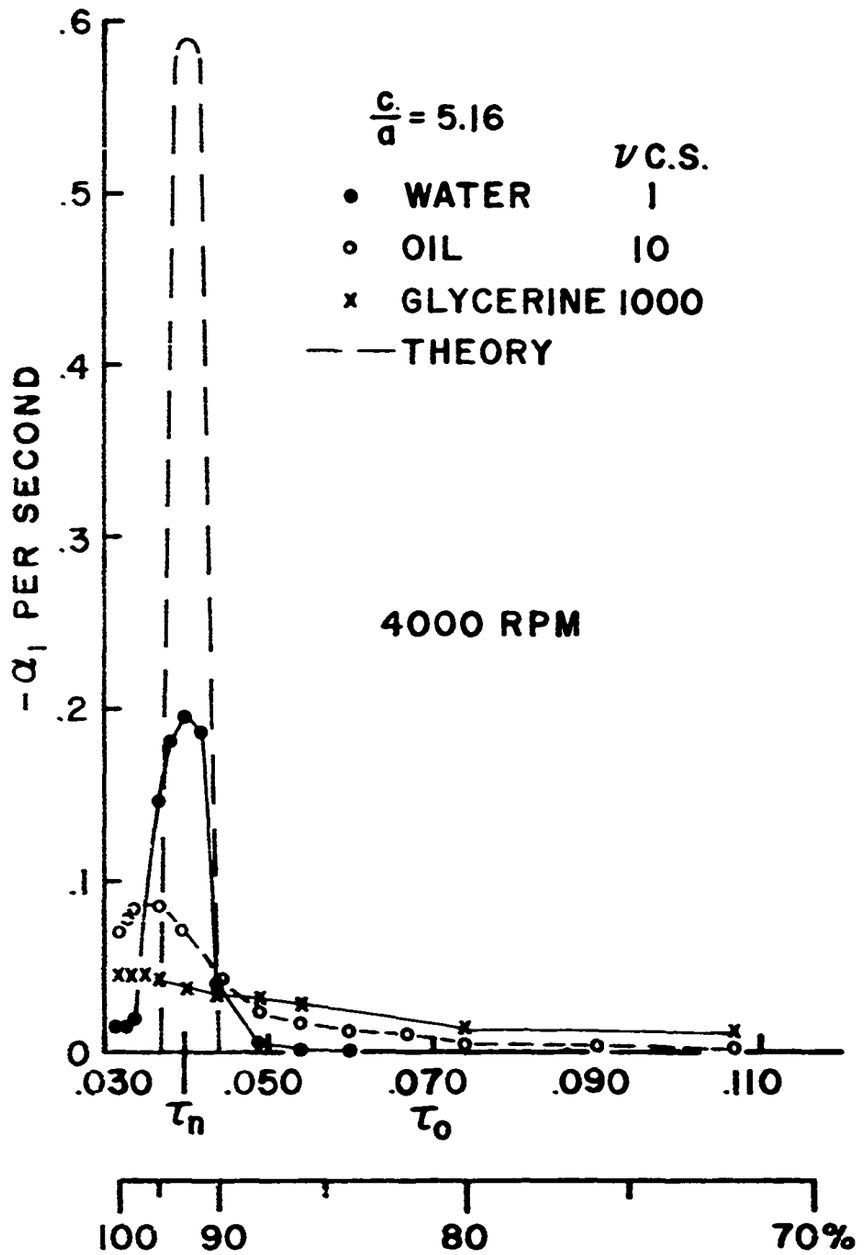

GYROSCOPIC SPIN RESULTS

FIG. 4

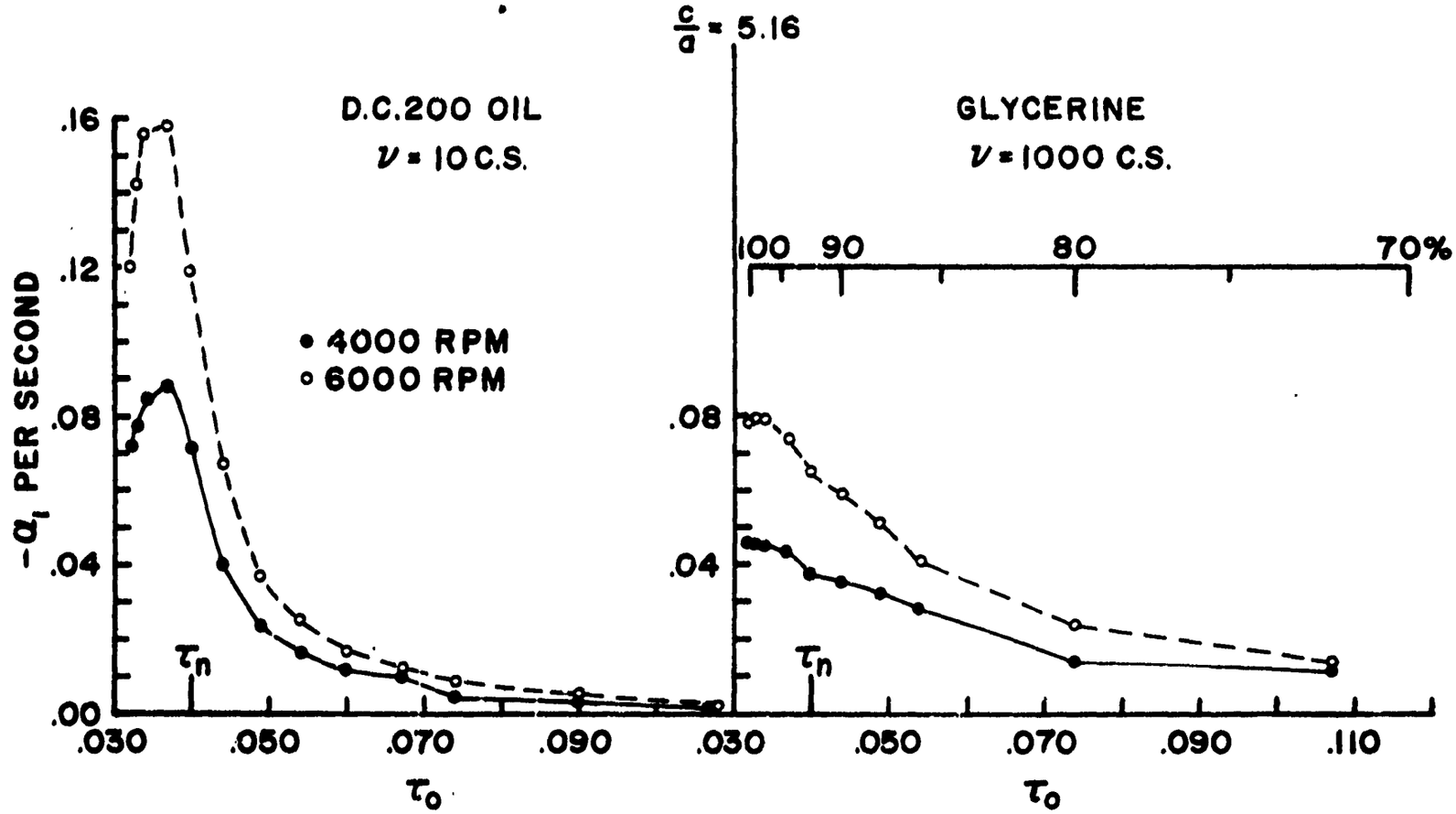

GYROSCOPIC SPIN RESULTS

FIG. 5

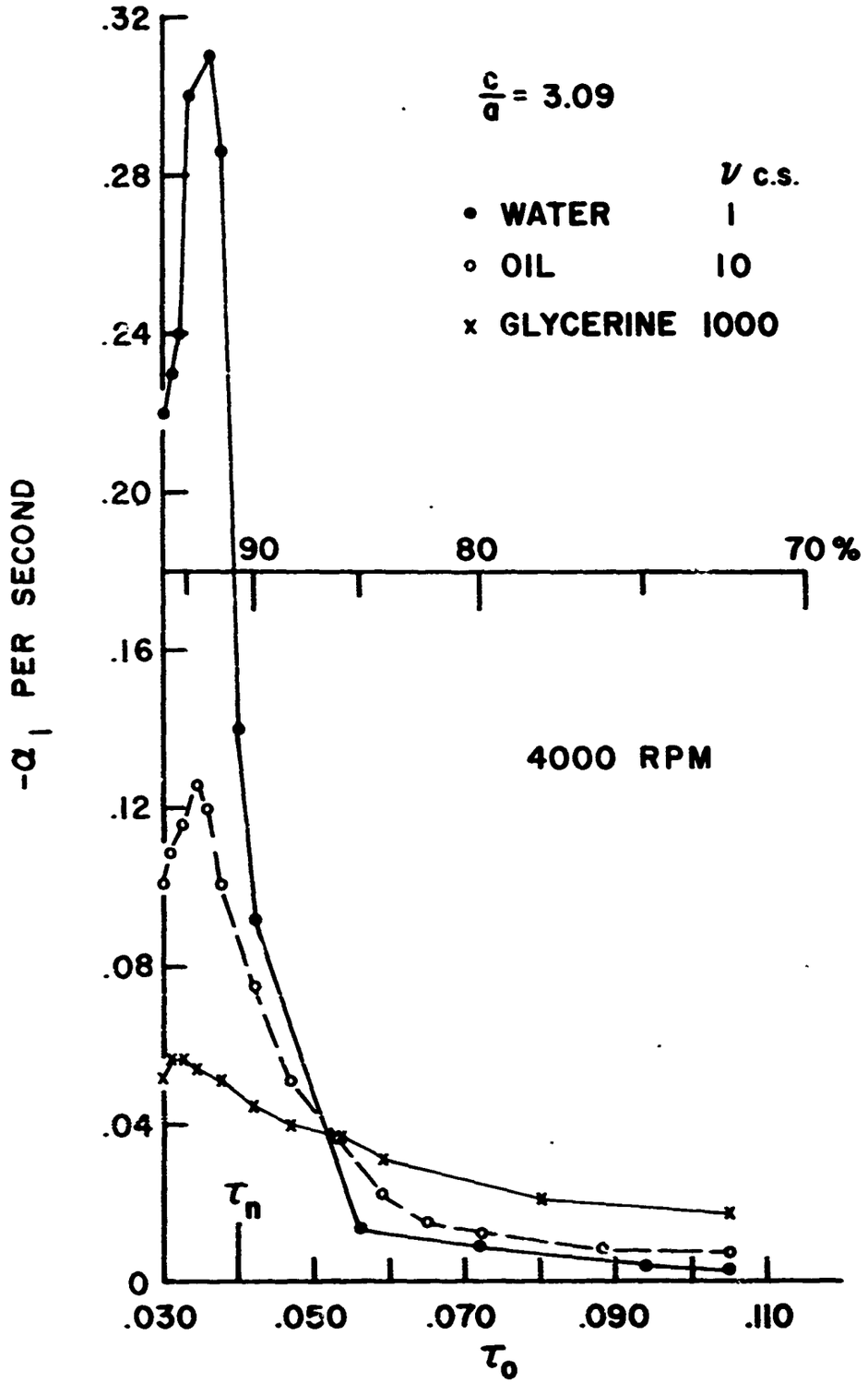

GYROSCOPIC SPIN RESULTS

FIG. 6

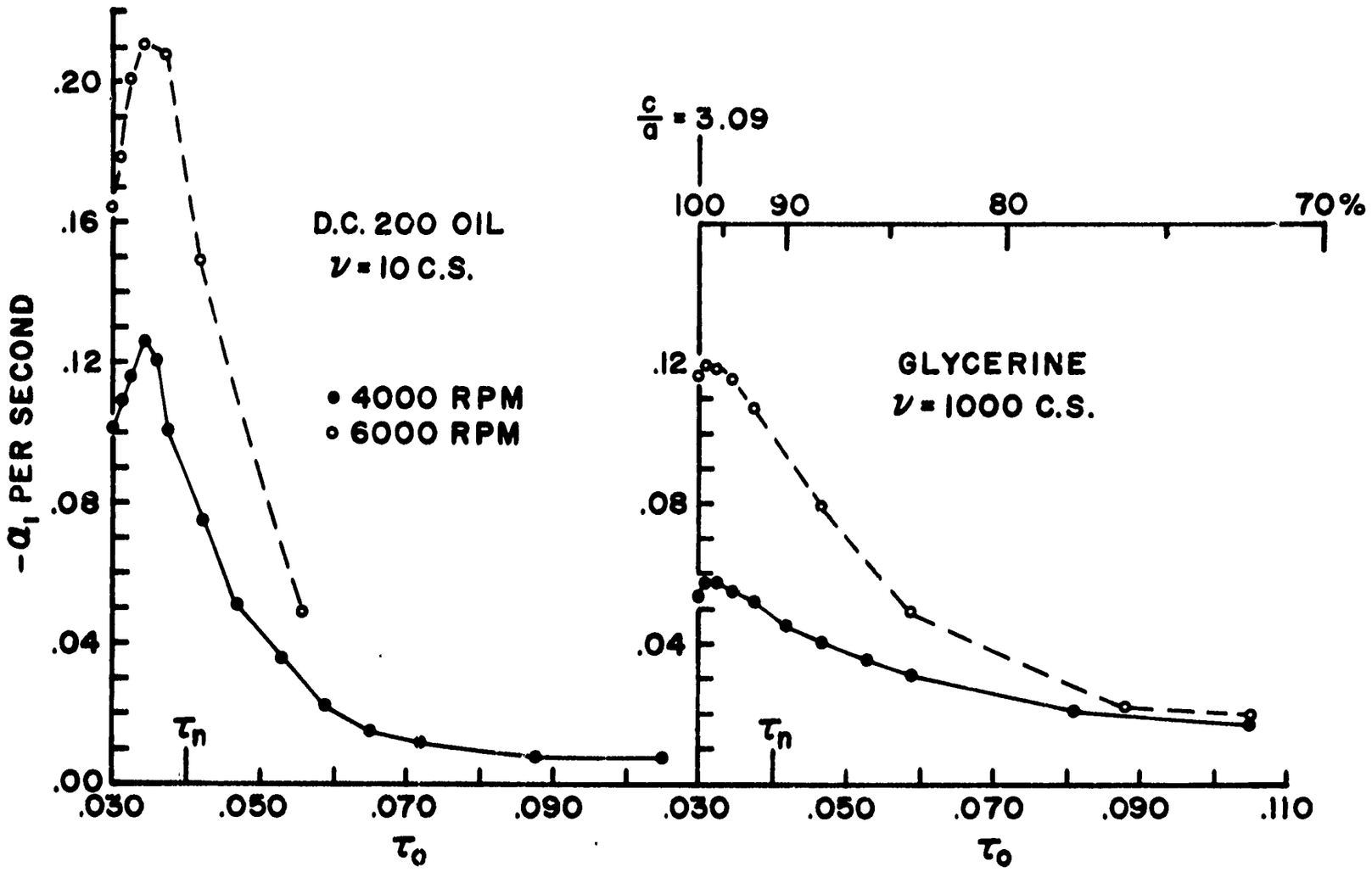

GYROSCOPIC SPIN RESULTS

FIG: 7

resonance to lower fill-ratios. The results are shown in Figure 8. For glycerine, the band is still truncated, but for oil, the response is symmetrical about its maximum.

4. DISCUSSION

Stewartson's theory of the instability of liquid-filled shell indicates that in the vicinity of coincidence (resonance) between one of the fluid frequencies, τ_o, and the nutational frequency of the shell, τ_n, the amplitude of the nutational component of yaw will grow as

$$e^{\alpha_1 t} \qquad (\alpha_1 \equiv \omega\tau)$$

where ω is axial spin of the shell and

$$\tau = 1/2 \sqrt{S - (\tau_o - \tau_n)^2}$$

$$S \equiv \frac{\rho(2R)^2 a^5}{I_x \sigma \; c/a} \qquad \text{"Stewartson's parameter"}$$

ρ = fluid density

2R is a tabulated function to be found in Stewartson's tables; it varies with τ_o and percent of fill.

a = radius of the cavity

$\sigma = \sqrt{1 - 1/s}$, s = gyroscopic stability factor.

For <u>instability</u>, τ must be real, or

$$S - (\tau_o - \tau_n)^2 > 0$$

which leads to the well known Stewartson <u>instability</u> criterion:

$$-1 < \frac{(\tau_o - \tau_n)}{S^{1/2}} < 1$$

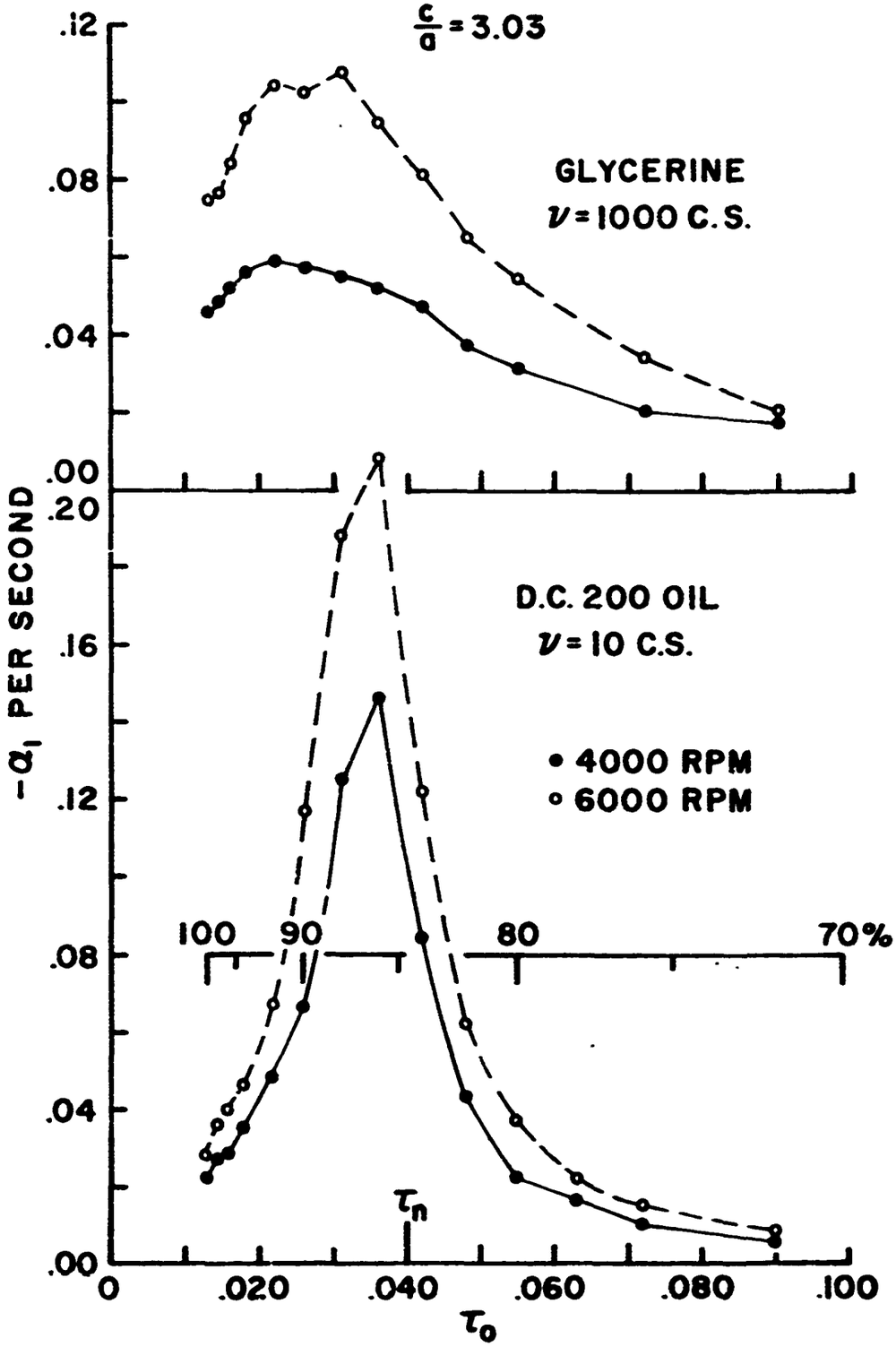

GYROSCOPIC SPIN RESULTS - SHORTENED CAVITY

FIG. 8

The half-width of the band of instability is

$$\Delta\tau = \sqrt{S}$$

The maximum rate of divergence is at exact resonance, $\tau_o = \tau_n$, for which

$$(\alpha_1)_{max} = \frac{\omega}{2}\sqrt{S} \qquad \text{per second.}$$

The theoretical curves were computed using these relations.

Observed results both in free flight and with gyroscope differ significantly from the predicted behavior. The differences appear to be:

(a) observed maxima of divergence are considerably lower than predicted and show marked dependence on viscosity

(b) the width of the resonance band also is considerably broader than predicted; the width increases with viscosity

(c) there appears to be a shift of $(\tau_o)_{max}$ relative to τ_n with viscosity.

It is instructive, as a first guess, to correlate these effects with Reynolds numbers.

4.1 Correlation with Reynolds Numbers:

We define the Reynolds number of the fluid in the cavity as:

$$Re = \frac{\omega a^2}{\nu}$$

The following are the Reynolds numbers of various tests:

	ν c.s.	Re	
Free Flight, Glycerine	1000	7.0×10^2	
Gyroscope:			
		4,000 rpm	6,000 rpm
Mercury	0.1	-	6.3×10^6
Water	1	4.2×10^5	6.3×10^5
Oil	10	4.2×10^4	6.3×10^4
Glycerine	1000	4.2×10^2	6.3×10^2

We shall consider the three observed differences in turn.

a. The Height at Resonance

The ratio of theoretical to observed rate of divergence at resonance

$$r = \frac{\alpha_{1\ th}}{\alpha_{1\ obs}},$$

is plotted vs. Re in Figure 9. Gyroscope results correlate quite well. From the trend of the correlation curve it would appear that an agreement with theoretical prediction would be attained at higher Reynolds numbers. An attempt, therefore, was made to test mercury. Tests with c/a = 3.09 and 3.03 cavities were unsuccessful because of violent divergence. Partial success was achieved in the c/a = 5.16 cavity. The results are shown in Figure 10. An extrapolation of the results to resonance, an uncertain procedure, suggests that the resonance would occur near τ_n, as predicted, and the rate of divergence, at resonance, would be close to the theoretically predicted value. However, if one incorporates into Figure 9 two other available data points: from free flight tests and Ward's result (see Appendix 4), these disagree with gyroscope results.

b. The Width of the Resonance Band

The resonance band shows progressive widening as viscosity increases. At higher viscosity it also exhibts surprisingly wide, almost non-terminating, tails. However, along these tails, the instability of the gyroscope is not self-generating but requires a bit of artificial help to start the nutational motion going. Once disturbed, the motion is divergent. With an empty cavity a similar initial disturbance invariably damped.

With such broad tails it is impractical to define the width of the band. For our purpose we define the width at one half of its maximum amplitude and compare this with theoretical width at corresponding height, i.e., $w = w_{1_{obs}} / w_{1_{th}}$ at 1/2 of $(\alpha_1)_{max}$. This ratio, so defined, is plotted vs. Re in Figure 11. Again, there is good correlation of gyroscope results but disagreement with free flight and Ward's values.

AT RESONANCE

$$r = \frac{\alpha_{i\,th}}{\alpha_{i\,obs}} \quad vs \quad Re$$

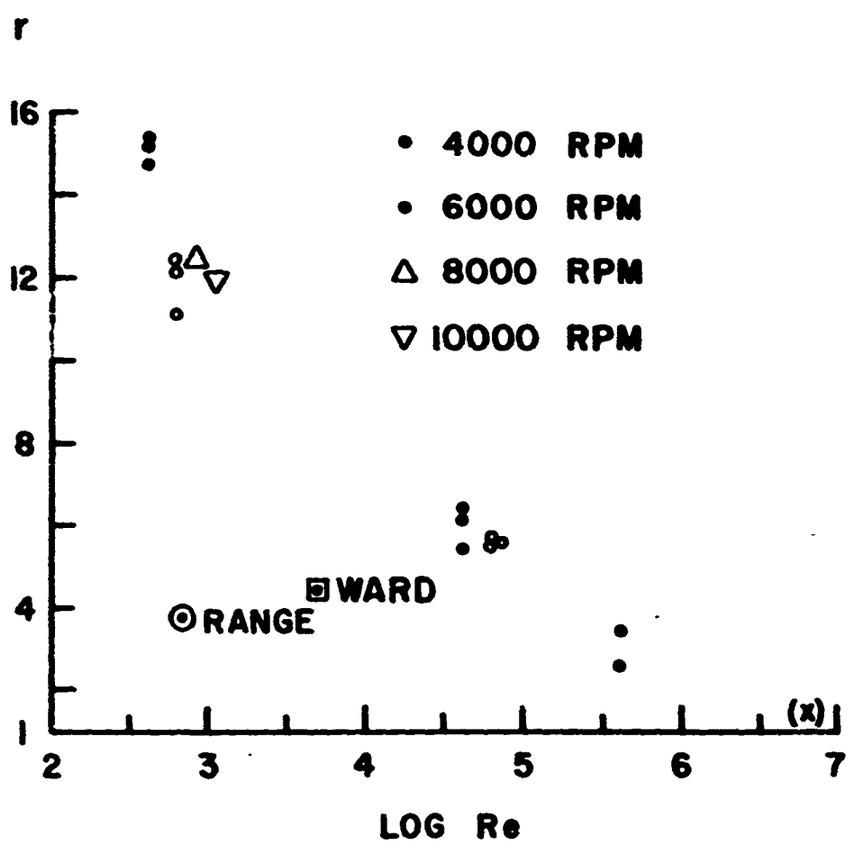

RATIO OF THEORETICAL TO OBSERVED RATE OF DIVERGENCE AT RESONANCE

FIG. 9

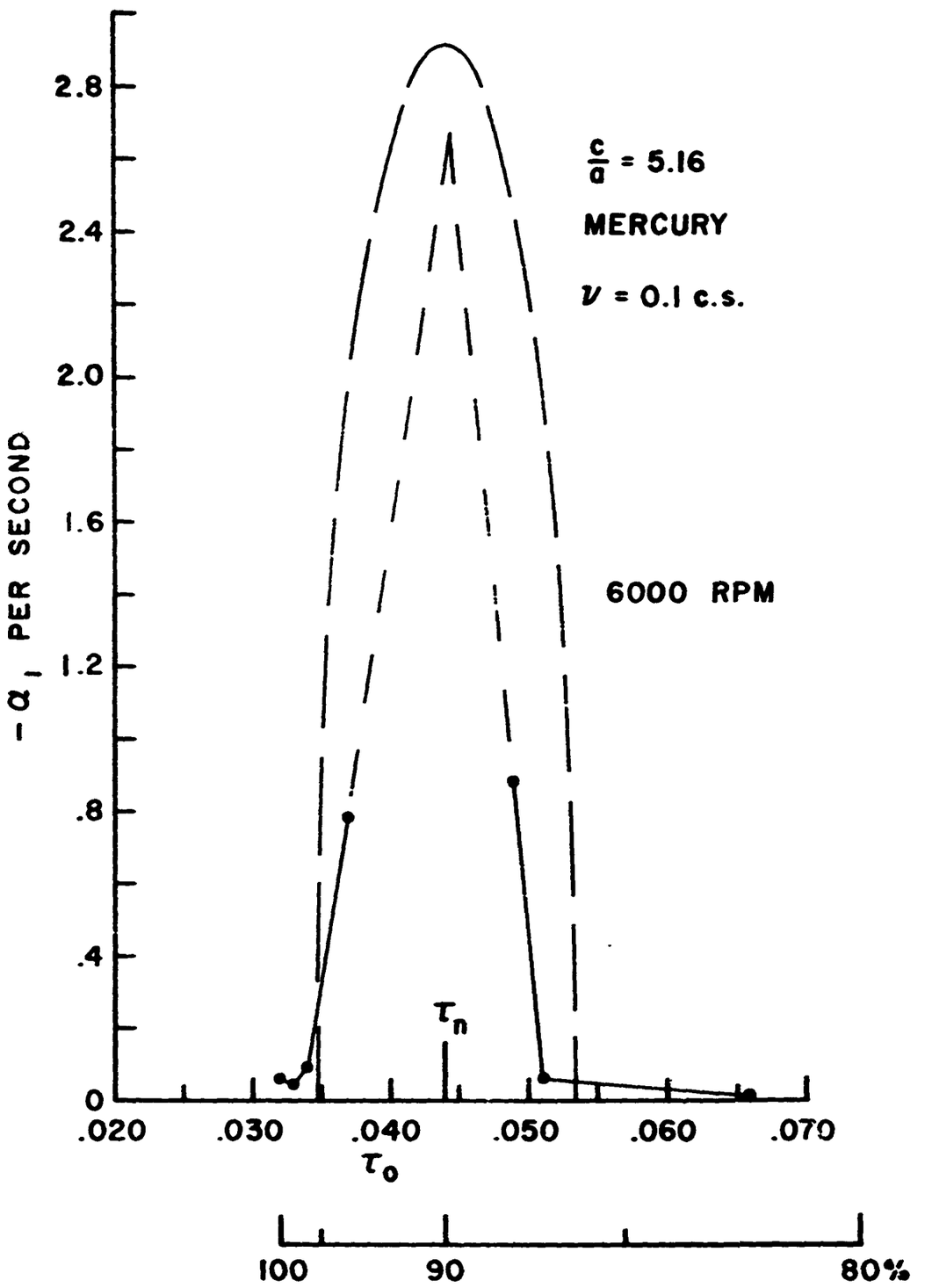

GYROSCOPIC SPIN TEST - MERCURY

FIG. 10

WIDTH OF BAND AT $\alpha_i = \frac{1}{2}(\alpha_i)_{max}$

$$W = \frac{W_1 \text{ obs}}{W_1 \text{ th}} \text{ vs Re}$$

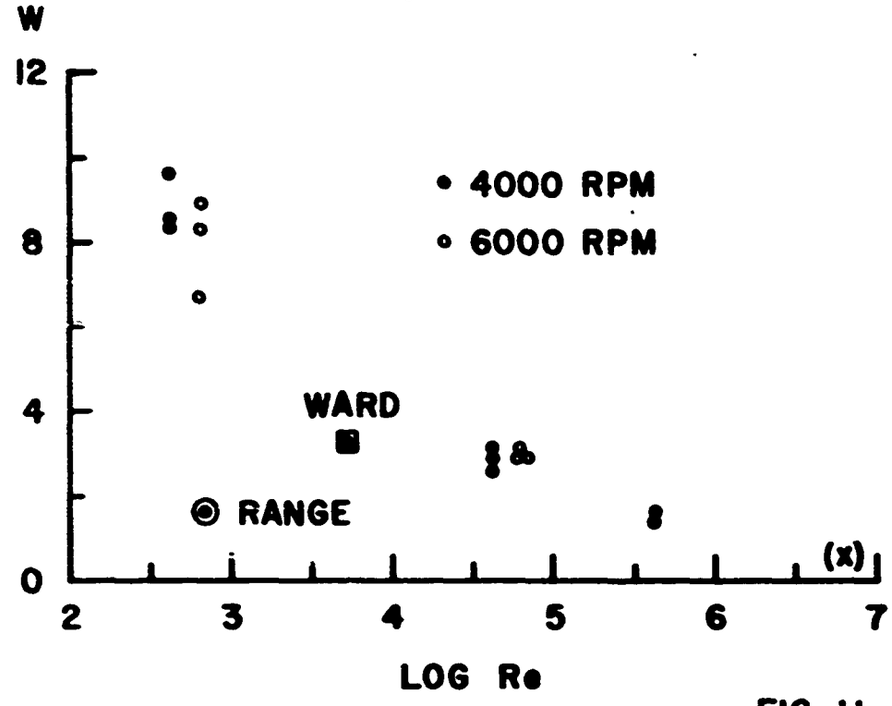

FIG. 11

SHIFT IN MAXIMA vs Re

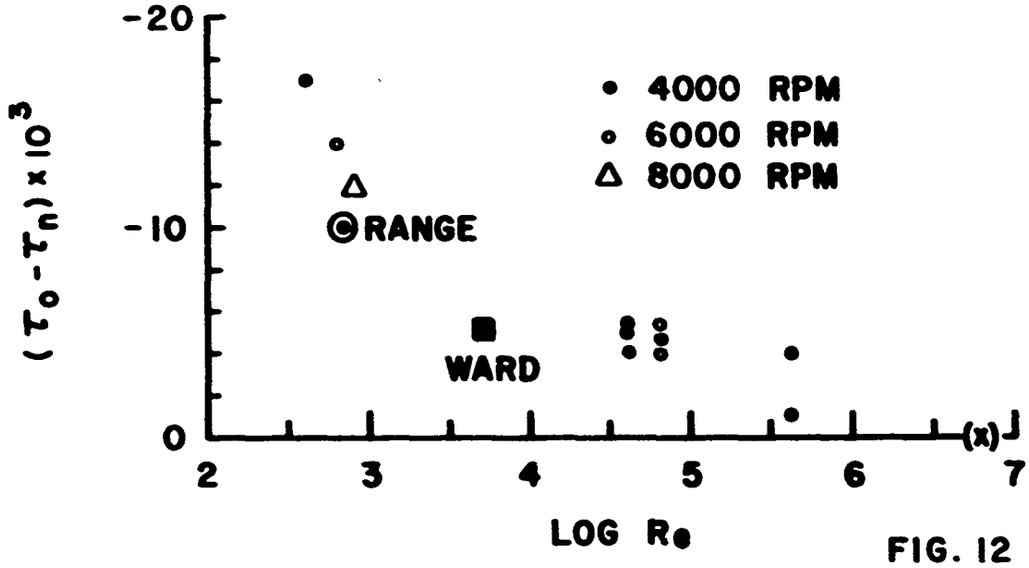

FIG. 12

c. Displacement of $(\tau_o)_{max}$ with Viscosity

Examination of the resonance graphs shows clearly that there is a progressive displacement of the observed peak of the resonance curve with viscosity. Thus, with glycerine, the peak occurs at $\tau_o = .026$ (c/a = 3.03) whereas the nutational frequency, $\tau_n = .040$, remains unchanged. In other fineness ratios, 5.16 and 3.09, the peaks are similarly displaced. However, in these cases the positions of the peaks for glycerine are quite uncertain and are omitted from the plot. The peak of other liquids also might be somewhat influenced by considerable asymmetry of the resonance curves.

The observed difference, $\tau_{o_{max}} - \tau_n$ is plotted vs. Re in Figure 12. In this case, the formerly discordant two data points, one from free flight and another from Ward, are in somewhat better agreement with gyroscope results.

The question may well be raised whether τ_n as modified by the inertial properties of the liquid (Appendix 3) is the appropriate reference, or should not τ_{n_o} of the empty system be used instead? With mercury, for example, the observed $\tau_n = .043$ whereas that of the empty gyroscope is $\tau_{n_o} = .036$. The resonance peak appears much closer to .043 than to .036. Also for glycerine the peak is at $\tau_o = .026$, whereas the observed $\tau_n = .040$ and that of the empty gyroscope is $\tau_{n_o} = .038$. The displacement is clearly present. For the case of free flight firings, the observed peak is at $\tau_o = .055$, whereas τ_{n_o} is .061 and with liquid .065. Thus, the displacement of $(\tau_o)_{max}$ appears to be real.

4.2 Viscous Damping:

Relatively good correlation of the gyroscope results, in the form of r, w, and $\Delta\tau$ with Reynolds numbers indicate the importance of viscosity. However, a significant disagreement between these results and r, w, and $\Delta\tau$ as obtained from the free flight and from Ward's experiments suggest that simple correlation with Reynolds numbers is inadequate.

To examine the effect of viscosity through the Navier-Stokes equations is very difficult. However, in general, the effect of viscosity on the oscillating fluid system is to act as an energy sink or a damper. In a mechanical analog this effect would be representable by a dash-pot. The solution for damped fluid oscillations, therefore, would contain imaginary components in all resonant frequencies terms. Any fluid frequency, therefore, would be of the form

$$\tau_o = \tau_{oo} + i\delta \tag{1}$$

where τ_{oo} is the resonant frequency of an inviscid fluid and δ is the damping factor of the τ_o mode.

From reference 3 or 5, the nutational root of the characteristic equation, defining the oscillations of the system, can be written

$$\tau - \tau_n = \frac{-S}{4(\tau - \tau_o)} \tag{2}$$

where S is the "Stewartson parameter" previously defined. The solution of this guadratic for τ leads to

$$\tau = \frac{\tau_o + \tau_n}{2} \pm \frac{i}{2}\sqrt{S - (\tau_o - \tau_n)^2} \ . \tag{3}$$

The nutational amplitude, in the absence of aerodynamic damping, is given by

$$\text{constant} \times e^{i\omega\tau t} \ .$$

For <u>instability</u> only the imaginary part of τ is important. Moreover, we must have

$$S - (\tau_o - \tau_n)^2 > 0 \quad ,$$

which is Stewartson's instability criterion, and take the negative sign in front of the square root.

With viscous damping, Equation (2) becomes

$$\tau - \tau_n = -\frac{S}{4(\tau - \tau_{oo} - i\delta)} \ . \tag{4}$$

The solution for τ becomes:

$$\tau = \frac{\tau_{oo} + \tau_n}{2} + \frac{i}{2}\left[\delta \pm \sqrt{S + \delta^2 - (\tau_{oo} - \tau_n)^2 - i\,2\delta(\tau_{oo} - \tau_n)}\right] \quad (5)$$

Let

$$m \equiv S + \delta^2 - (\tau_{oo} - \tau_n)^2$$

$$n \equiv 2\delta(\tau_{oo} - \tau_n) \ .$$

The real negative part of the imaginary component of complex τ is:

$$1/2\left[\sqrt{\frac{m + \sqrt{m^2 + n^2}}{2}} - \delta\right] \ . \quad (6)$$

At resonance, i.e., when $\tau_{oo} - \tau_n = 0$, Equation (6) becomes particularly simple. Call this viscous τ_v

$$\tau_v = 1/2\left[\sqrt{S + \delta^2} - \delta\right] \ . \quad (7)$$

The inviscid τ_i is

$$\tau_i = 1/2\sqrt{S} \ . \quad (8)$$

a. The Amplitudes

The problem now is to determine δ from the experiments. We assume that the observed ratio of amplitudes, r, is equal to the ratio of inviscid to viscous τ's, i.e.,

$$r = \frac{\alpha_{1\ th}}{\alpha_{1\ obs}} = \frac{\tau_i}{\tau_v} = \frac{\sqrt{S}}{\sqrt{S + \delta^2} - \delta} \ . \quad (9)$$

From Equation (9)

$$\delta = 1/2\sqrt{S}\left(r - \frac{1}{r}\right) \ . \quad (10)$$

The following table summarizes the values of r, w, and $\Delta\tau$ previously plotted in Figures 9, 11, and 12. In the case of $\Delta\tau$ only the averages are given.

Observed r, w, $\Delta\tau$

Source	$\sqrt{S}$	r		w		$-\Delta\tau \times 10^3$
Range	1.37×10^{-2}	3.7		2.3		10
Ward	0.87×10^{-2}	4.4		3.3		5
Gyroscope:		4000 rpm	6000 rpm			
Hg	13.69×10^{-3}	-	(1.4)	-	(1)	(0)
H_2O	3.71×10^{-3}	2.8	-	1.4	-	2
Oil	3.71×10^{-3}	5.9	5.6	3.0	2.9	5
Glycerine	4.16×10^{-3}	15.1	11.9	8.7	8.1	16

For the gyroscope, the values of $\sqrt{S}$ are those for c/a = 3.09.

A plot of log δ vs. log Re suggested*

$$\delta = \frac{\text{const.}}{(\text{Re})^n} \quad .$$

Because of the distribution of the data, neither the constant nor the value of n could be well determined. However, the following values represent the data reasonably well.

$$n = 1/4$$

$$\text{constant} = 0.135 \pm .017 \text{ s.d.}$$

A comparisen of computed τ_i/τ_v ("predicted") with the observed r is shown in Figure 13a. There are some indications that at lower Reynolds numbers, for $\text{Re} < 10^5$, the exponent n might be 1/5 and be more nearly 1/2 at higher Reynolds numbers. But present data are insufficient to make this distinction.

---

* *The form of dependence of δ on Reynolds numbers was suggested by Wedemeyer on Theoretical grounds, see Reference 6.*

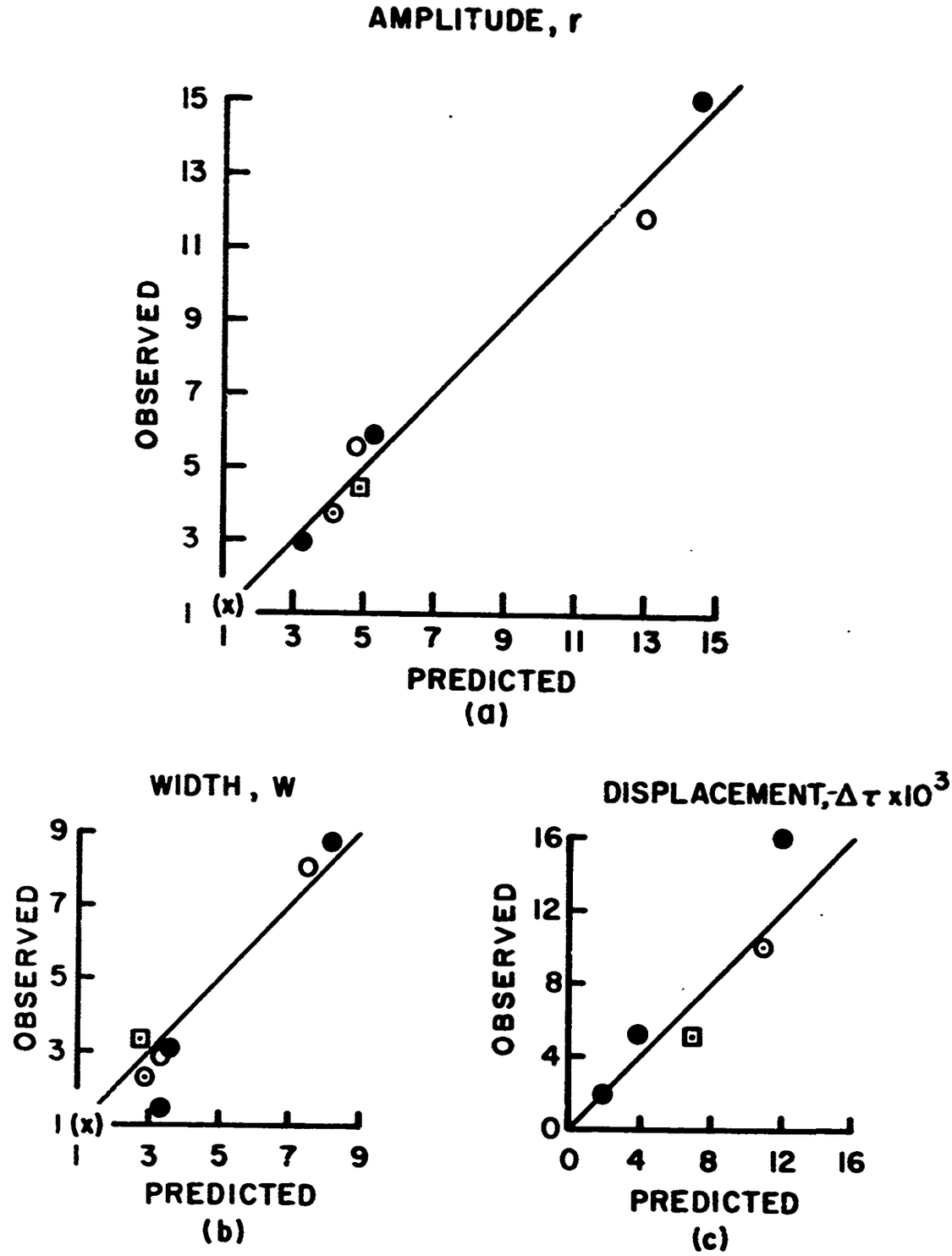
AMPLITUDE, r
OBSERVED
PREDICTED
(a)
WIDTH, W
OBSERVED
PREDICTED
(b)
DISPLACEMENT, -Δτ x10^3
OBSERVED
PREDICTED
(c)

FIG. 13

b. The Width

In contrast to the inviscid solution which exhibits definite band width, $2\sqrt{S}$, the viscous solution, Equation (6), shows tails whose amplitudes only asymptotically approach zero. Hence, it is impractical to define the resonance band width. However, a very simple expression for characteristic width can be obtained if we neglect m^2 relative to n^2 under the square root of Equation (6). Such characteristic width, then, can be defined by the following equation:

$$\sqrt{\frac{S + \delta^2 - (\tau_{oo} - \tau_n)^2 + 2\delta(\tau_{oo} - \tau_n)}{2}} - \delta = 0 \ . \qquad (11)$$

From this it follows that the viscous half-width, is

$$w_v = \sqrt{S} + \delta \ . \qquad (12)$$

The inviscid half-width is

$$w_i = \sqrt{S} \ .$$

The ratio $w = w_v/w_i = 1 + \delta/\sqrt{S}$, or

$$\delta = \sqrt{S}\,(w - 1) \ . \qquad (13)$$

The width, w_v, Equation (12) occurs from one third to one half of the maximum amplitude. This depends on the value of $\delta/\sqrt{S}$. Therefore, the ratio $w = w_v/w_i$ is not strictly comparable to the previously used ratio w at one half of the maximum amplitude. Nevertheless, the two are compared in Figure 13b. For "predicted" values, w_v/w_i, previously found $\delta = .135/\sqrt[4]{Re}$ was used. The agreement is fair.

c. Displacement of $(\tau_o)_{max}$

Interaction between oscillating fluid particles and the walls of the cavity apparently gives rise to the boundary layer. This boundary layer, in turn, may produce an "effective" fineness ratio of the cavity, slightly different from the geometrical. A rough estimate of this effect can be made as follows.

Let c/a be the geometrical fineness ratio. If the boundary layer has thickness y, the "effective" ratio will be

$$\frac{c - y}{a - y} \quad .$$

The difference is

$$\Delta\left(\frac{c}{a}\right) = \frac{c}{a} - \frac{c - y}{a - y} = - \frac{\left(\frac{c}{a} - 1\right) \frac{y}{a}}{1 - \frac{y}{a}} \quad . \tag{14}$$

From Stewartson's tables one finds that a change $\Delta\left(\frac{c}{a}\right)$ produces a change $\Delta\tau_o$. The two are related by

$$\Delta\left(\frac{c}{a}\right) \doteq 1.2(2j + 1)\, \Delta\tau_o \quad . \tag{15}$$

Equating Equations (14) and (15), the desired answer is

$$\Delta\tau_o \doteq - \frac{\left(\frac{c}{a} - 1\right)}{1.2(2j + 1)} \left(\frac{y}{a}\right) \quad . \tag{16}$$

Since $\Delta\tau_o$ is known from observations, $\left(\frac{y}{a}\right)$ can be computed and plotted vs. Re. The results are:

$$\Delta\tau_o = \tau_{oo} - \tau_n \doteq - \frac{c/a - 1}{2j + 1} \times \frac{.086}{\sqrt[4]{Re}} \quad . \tag{17}$$

A plot of "predicted" $\Delta\tau_o$, computed by Equation (17), vs. observed is shown in Figure 13c. The agreement is tolerable.

Finally, it is of interest to compare the observed resonance band with that theoretically predicted with viscous damping included. The theoretical curve was computed using Equation (6), i.e.,

$$(\alpha_1)_{\text{theory}} = \frac{\omega}{2} \left[\sqrt{\frac{m + \sqrt{m^2 + n^2}}{2}} - \delta \right]$$

with

$$\delta = \frac{.135}{\sqrt[4]{Re}}$$

and compared with the observed α_1's for oil, Figure 8, c/a = 3.03, 6000 rpm. The comparison is given in Figure 14. The agreement is excellent. Particularly noteworthy is the theoretical appearance of wings in the resonance band which were so conspicuous in gyroscope experiments with more viscous fluids. Therefore, introduction of viscous damping clearly improves the inviscid theory when applied to real fluids.

5. CONCLUDING REMARKS

Stewartson's inviscid theory still provides the best available guide for predicting a priori the dynamic behavior of liquid carrying shell with cylindrical cavity. It is suggested, however, that shell designers will do better by taking into account the effects of viscosity of their fluids. The following steps outline the procedure to be followed.

a. Nutational frequency: This to be computed by taking inertial properties of the liquid into account.

$$\tau_n = 1/2 \frac{I_x}{I_y} (1 + \sigma) \tag{18}$$

where

$$I_x = I_{x_o} + i_{x_o} \tag{19}$$

$$I_y = I_{y_o} + 0.7\, i_{y_o} \cdot$$

I_{x_o}, I_{y_o} are the axial and transverse moments of inertia respectively of the empty shell and i_{x_o} and i_{y_o} are those of the fluid regarded as a rigid body.

b. The maximum divergence will occur at the principal fluid frequency given by

$$\tau_{o_{max}} = \tau_n - \Delta\tau \tag{20}$$

where

$$\Delta\tau = \frac{c/a - 1}{2j + 1} \frac{.086}{\sqrt{Re}} \cdot \tag{21}$$

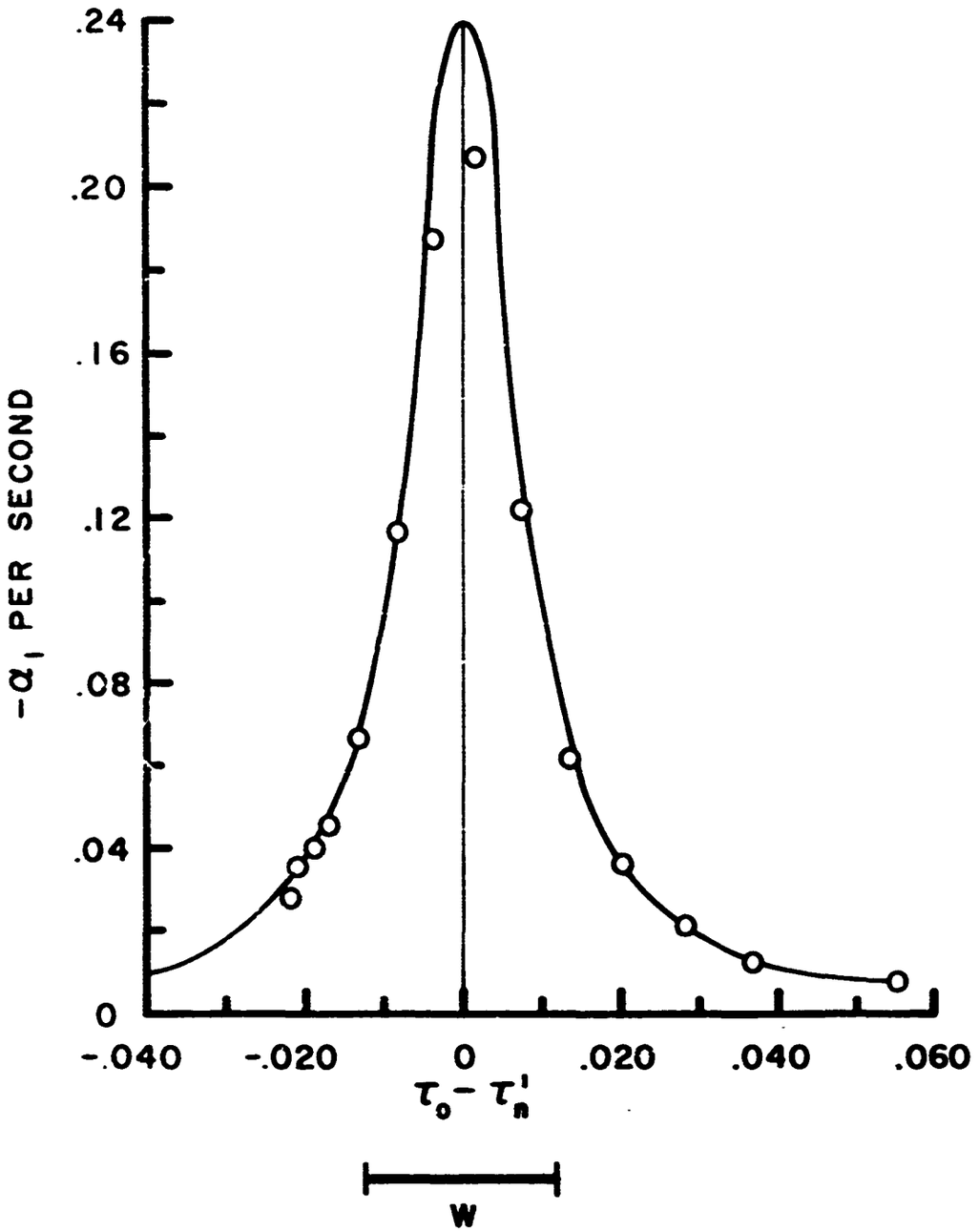

—— MODIFIED THEORY

o OBSERVED: TRANSPOSED FROM FIG. 8

$\frac{c}{a} = 3.09$, ν 10 c.s., 6000 R.P.M.

FIG. 14

c. From Stewartson's tables one finds the value of $(c/a)/(2j + 1)$ corresponding to above $\tau_{o_{max}}$. Let this be K_o. Therefore,

$$(c/a)_o = K_o(2j + 1) \quad .$$

These are the fineness ratios of the cavities at which maximum instability will occur.

d. Because of the width of the resonance band, the designer should avoid fineness ratios in the vicinity of the critical $(c/a)_o$. Half-width of the resonance band is

$$\tau_o - \tau_{o_{max}} = \sqrt{S} + \delta \quad .$$

Therefore, one should find from the tables the limiting fineness ratios corresponding to

$$\tau_o = \tau_{o_{max}} \pm (\sqrt{S} + \delta) \quad . \tag{22}$$

Roughly, this is given by

$$\Delta(\frac{c}{a}) = 1.2(2j + 1)(\sqrt{S} + \delta) \quad . \tag{23}$$

Therefore, the fineness ratios to be avoided are

$$(\frac{c}{a})_o \pm \Delta(\frac{c}{a}) \quad . \tag{24}$$

It should be noted that the inviscid instability criteria

$$-1 < \frac{\tau_o - \tau_n}{\sqrt{S}} < 1$$

with viscous correction becomes

$$-(1 + \frac{\delta}{\sqrt{S}}) < \frac{\tau_o - \tau_n}{\sqrt{S}} < (1 + \frac{\delta}{\sqrt{S}}) \tag{25}$$

where

$$\delta = \frac{.135}{\sqrt[4]{Re}}$$

$$Re = \frac{\omega a^2}{\nu} \quad .$$

An example: From our range firings, $\tau_n = .065$. From Equation (21), $\Delta\tau = .011$. Therefore, the maximum divergence will occur at fluid frequency $\tau_{o_{max}} = .065 - .011 = .054$. From Stewartson's tables for $b^2/a^2 = 0.10$ (90 percent fill) we find

$$\frac{c/a}{2j + 1} = 1.044 = K_o$$

for

$$j = 1$$

$$(c/a)_o = 3.13 \quad .$$

For this shell,

$$\sqrt{S} = 1.37 \times 10^{-2}$$

$$\delta = 2.63 \times 10^{-2}$$

$$\therefore \sqrt{S} + \delta = .040$$

and by Equation (24), the range of fineness ratios to be avoided

$$3.13 \pm .14$$

or from c/a = 2.99 to c/a = 3.27. From Figure 2 and tables we obtain the following:

Lower limit	$\tau_o = .020$	c/a = 3.09
Upper limit	$\tau_o = .090$	c/a = 3.27 .

These numbers are in a fair agreement with the estimates by using Equation (23).

With slightly greater sophistication, the width of the resonance band, or the range of (c/a) values about the critical should be determined relative to aerodynamic damping. Only the rate of divergence of the nutational component of yaw which is in excess of the rate due to aerodynamic damping is important in practice. If, therefore, α_o is the aerodynamic damping rate, then the width of the resonance band is to be found from the condition

$$\frac{\omega}{2}\left[\sqrt{\frac{m + \sqrt{m^2 + n^2}}{2}} - \delta\right] = \alpha_o \qquad (26)$$

where

$$m = S + \delta^2 - (\tau_o - \tau_{om})^2$$

$$n = 2\delta(\tau_o - \tau_{om})$$

$$\tau_{om} = \tau_n - \Delta\tau \ .$$

From this one finds lower and upper τ_o and, from the tables, corresponding fineness ratios.

ACKNOWLEDGEMENTS

The author is grateful to Mr. E. H. Wedemeyer for suggesting the approach for handling viscous damping and to Mr. B. McKay for performing all gyroscope experiments.

B. G. KARPOV

6. REFERENCES

1. Karpov, B. G. Experimental Observations of the Dynamic Behavior of Liquid-Filled Shell. BRL Report 1171 (August 1962).

2. Wedemeyer, E. H. The Unsteady Flow Within a Spinning Cylinder. J. Fluid Mech., 20, Part 3 (November 1964).

3. Stewartson, K. On the Stability of Spinning Top Containing Liquid J. Fluid Mech., 5, Part 4 (1959).

4. Murphy. C. H., Schmidt, L. E. The Effect of Length on the Aerodynamic Characteristics of Bodies of Revolution in Supersonic Flight. BRL Report 876 (August 1953).

5. Karpov, B. G. Dynamics of Liquid-Filled Shell, Aids for Designers. BRL Memorandum Report 1477 (May 1963).

6. Wedemeyer, E. H. Dynamics of Liquid-Filled Shell: Theory of Viscous Corrections to Stewartson Stability Problem. BRL Report 1287, (June 1965).

7. Arnold. R. N., Maunder, L. Gyrodynamics and Its Engineering Applications. Academic Press (1961).

8. Scott, W. E. The Free Flight Stability of a Liquid-Filled Shell, Part Ia. BRL Report 1120 (December 1960).

APPENDIX 1

PHYSICAL AND DYNAMIC CHARACTERISTICS OF 20mm MODELS

21 models were fired in this program. Since their inferred characteristics showed no systematic variation with fineness ratios of the cavities, all results were combined. All errors assigned to the mean values are standard errors.

Rotational Frequency $\varphi_1' = .0271 \pm .0004$ rad/cal

Precessional Frequency $\varphi_2' = .0060 \pm .0001$ rad/cal

$$\frac{I_x \nu}{I_y} = \varphi_1' + \varphi_2' = .0331 \pm .0004 \text{ rad/cal}$$

$$\nu = .415 \text{ rad/cal}$$

$$\frac{I_x}{I_y} = .0797 \pm .0011$$

$$\sigma = \frac{\varphi_1' - \varphi_2'}{\varphi_1' + \varphi_2'} = .640 \pm .012$$

$$\therefore \tau_2 = \frac{I_x}{2I_y}(1+\sigma) = .065 \pm .001$$

From physical measurements of empty models prior to firings,

$$\frac{I_{y_0}}{I_{x_0}} = .0747$$

which, with the above σ, gives $\tau_{2_0} = .061$. The difference between empty $\frac{I_{y_0}}{I_{x_0}}$ and the dynamic $\frac{I_x}{I_y}$, as inferred from firings, is due to the effect of the inertial properties of the liquid.

Also:

$$C_{M_\alpha} = 3.66 \pm .06$$

and

$$s = \frac{1}{1-\sigma^2} = 1.69 \pm .02 = \frac{I_x^2 \nu^2}{2I_y \rho S d^3 C_{M_\alpha}}$$

Knowing the rates, one can determine I_x and I_y separately.

Let

$$I_x = I_{x_o} + \alpha i_{x_o}$$

$$I_y = I_{y_o} + \beta i_{y_o}$$

where i_{x_o} and i_{y_o} refer to the liquid acting as a rigid body. We have:

$$I_{x_o} = 24.81 \text{ gm-cm}^2 \qquad i_{x_o} = 2.74 \text{ gm-cm}^2$$

$$I_{y_o} = 332.09 \text{ gm-cm}^2 \qquad i_{y_o} = 17.68 \text{ gm-cm}^2$$

The firings indicate that

$$\alpha = .96$$

$$\beta = .70$$

All firings were done at 2000 fps from a gun with a twist of rifling 1:15. Other aerodynamic characteristics of the models are:

C_D	.350	Wt 44.4 gms
C_{L_α}	2.47	
$C_{M_{p_\alpha}}$	.30	
$C_{M_q} + C_{M_{\dot{\alpha}}}$	-12.0	
C_{f_p}	-.012	

Damping rates:

Nutation $\alpha_1 = 3.20 \times 10^{-4}$ per caliber, $e^{-\alpha_1 p}$

Precession $\alpha_2 = 2.54 \times 10^{-4}$ per caliber

APPENDIX 2

THEORY OF GYROSCOPE

This theory is sufficiently well known not to require full exposition here, see, for example, reference 7. However, a few brief remarks may be useful.

Let I_y be the polar moment of inertia of the rotor

I_y, I_y', I_y'' be the transverse moments of inertia of the rotor, inner and outer gimbals respectively, about the y axis

I_z, I_z' similarly about z axis. Clearly, $I_z'' = 0$.

Let $I_{y_o} = I_y + I_y' + I_y''$

$I_{z_o} = I_z + I_z'$

Then, if the gyroscope is so designed that

$I_{y_o} \approx I_{z_o}$ let,

$I = \sqrt{I_{y_o} I_{z_o}}$ be the moment about either axis.

Let us assume that bearing friction can be represented as $f_y \dot{\theta}_y$ and $f_z \dot{\theta}_z$ respectively. Moreover, if $f_y \doteq f_z$, as was the case with our bearings, then the differential equations of motion can be written as:

$$\begin{aligned} I\ddot{\theta}_y + f\dot{\theta}_y + I_x n\dot{\theta}_z - K_o\theta_y &= 0 \\ I\ddot{\theta}_z + f\dot{\theta}_z - I_x n\dot{\theta}_y - K_o\theta_z &= 0 \end{aligned} \tag{1}$$

where n is constant spin in rad/sec, and $K_o \equiv gMh$ is gravitational moment. M is the mass of the rotor and the inner gimbal and h is the center of mass-pivot separation. For the unstable position, i.e., when c.m. is above the pivot, $K_o > 0$.

Define: $\theta = \theta_Y + i\,\theta_Z$

The two equations can be combined to give

$$I\ddot{\theta} + (f - i\,I_x n)\dot{\theta} - K_o\theta = 0 \qquad (2)$$

where $i = \sqrt{-1}$.

The characteristic equation of (2) is

$$I m^2 + [f - i\,I_x n]m - K_o = 0$$

The roots are complex giving two frequencies and two damping rates.

With an approximation that $f/I_x n \ll 1$, these are

	Frequencies	Damping Rates
Nutation	$\frac{I_x n}{2I}(1+\sigma)$	$-\frac{f}{2I}(1+\sigma)$
Precession	$\frac{I_x n}{2I}(1-\sigma)$	$-\frac{f}{2I}(1-\sigma)$

where $\sigma = \sqrt{1 - \frac{1}{s}}$

$s = \frac{I_x^2 n^2}{4IK_o}$ gyroscopic stability factor.

Non-dimensional frequencies are

$$\tau_n = \frac{I_x}{2I}(1+\sigma)$$

$$\tau_p = \frac{I_x}{2I}(1-\sigma)$$

If $\sigma \sim 1$, s is large, $\tau_n \doteq \frac{I_x}{I}$ and

$$\sigma = 1 - \frac{1}{2s} + \ldots$$

$$\tau_p \doteq \frac{I_x}{2I}\,\frac{1}{2s} = \frac{K_o}{I_x n^2}$$

It should be noted that if $K_c < 0$, statically stable position, $s < 0$,

$\sigma > 1$ and the precessional amplitude has a tendency to diverge at a rate depending on the quality of the bearing or on the value of f. For statically unstable configuration, $K_o > 0$, $s > 0$ and $\sigma < 1$, friction damps both amplitudes.

If we introduce into one component, say θ_y, an additional stabilizing torque, -K, due to measuring device, the equations become

$$I\ddot{\theta}_y + I_x n\dot{\theta}_z - (K_o - K)\theta_y = 0$$

$$I\ddot{\theta}_z - I_x n\dot{\theta}_y - K_o\theta_z = 0$$

where friction, which does not affect the frequencies, was neglected.

It can be shown that, in this case, the new frequencies are:

$$\tau_n \triangleq \frac{I_x}{I} \text{ as before, and}$$

$$\tau_p \triangleq \frac{\sqrt{(K_o - K)K_o}}{I_x n^2}$$

APPENDIX 3

CONTRIBUTION OF LIQUID TO THE INERTIAL PROPERTIES OF THE SYSTEM

Both in free flight and gyroscope experiments with liquids the observed nutational frequency was always somewhat <u>higher</u> than for the empty system. The liquid, therefore, must have contributed its inertial properties to the system. From free flight experiments it was found that the liquid contributed 96 percent of its axial moment and 60 percent of its transverse moments of inertia when considered as an equivalent rigid body.

The gyroscope offered an opportunity to find the liquid's contribution with greater accuracy. The obvious choice of fluid is mercury for which

$$\frac{i_{x_o}}{I_{x_o}} = .75$$

$$\frac{i_o}{I_o} = .60$$

Again, we define:

$$I_x = I_{x_o} + \alpha\, i_{x_o}$$

$$I = I_o + \beta\, i_o$$

where I_{x_o}, I_o and i_{x_o}, i_o are the axial and transverse moments of inertia of the rotor and of the liquid considered as a rigid body, respectively.

From Appendix 2, it is easily seen that

$$\frac{I_x}{I} = (\tau_n + \tau_p)$$

$$\frac{K}{I_x} = (\tau_n + \tau_p)\frac{n^2}{4s}$$

$$\frac{K}{I} = (\tau_n + \tau_p)^2 \frac{n^2}{4s}$$

and

$$\sigma = \frac{\tau_n - \tau_p}{\tau_n + \tau_p} = \sqrt{1 - \frac{1}{s}}$$

The frequencies are directly observable quantities. If one knows I_{x_o}, and I_o and the moment $\underline{K}$ from prior physical measurements, then, by experiments, one determines I_x and I, and, hence, α and β. A series of experiments were run for this purpose and the results are given in the following table:

Dynamic Properties of Mercury-Filled Gyroscope

c/a = 5.16

% Fill	Spin rpm x 10^{-3}	$\frac{I_x}{I}$	α	β
100	2.5	.0437	.97	.69
	4.0	.0419	.98	.82
90	4.0	.0454	.97	.74
85	3.0	.0456	.97	.67
	4.0	.0451	.95	.68
	6.0	.0446	.94	.69
80	3.0	.0456	.96	.68
75	3.0	.0458	.95	.67
		Average	.96	.70
Empty		.0359		

Although the exact agreement of average α and β with free flight value. is fortuitous, the experiments indicate that the axial moment

of the empty system is fully augmented by the axial moment of the liquid, considered as a rigid body, and the transverse moment by 70 percent. The latter value appears to be in good agreement with the theoretical value for an inviscid fluid[8]. In the inviscid theory, there is no contribution by the liquid to the axial moment of inertia of the system.

APPENDIX 4

WARD'S EXPERIMENTS

Ward [5] tested Stewartson's theory with a gyrostat by varying fill-ratios in a fixed cylindrical cavity.

It is to be recalled that Stewartson's instability condition is:

$$-1 < \frac{(\tau_o - \tau_n)}{S^{\frac{1}{2}}} < 1$$

Ward found that the following limits best satisfy his observations:

$$-3.9 < \frac{(\tau_o - \tau_n)}{S^{\frac{1}{2}}} < 2.7$$

Thus, the limits are considerably broader than predicted and asymmetric relative to τ_n. However, he did find that maximum instability appeared to coincide with the predicted position at 66 percent fill-ratio.

From the cited reference, the characteristics of the gyrostat are:

Cavity: $a = 1.43$ cm

$c/a = 3.00$

Volume = 55 cc

Nutational frequency, $\tau_n = .112$

Fluid: $\nu = 23.9$ c.s.

$\rho = 1.2$ gm/cc (assumed)

Spin 6,000 rpm

Re = 5.4×10^3

With above characteristics of the cavity and $\tau_n = .112$ we find, from Stewartson's tables at $\tau_c = \tau_n$, $2R = .308$ (Stewartson's R). Therefore

$$S^{-\frac{1}{2}} = 114.3$$

Thus,

$$-3.9 < 114.3(\tau_o - \tau_n) < 2.7$$

it follows:

	τ_c	b^2/a^2	% fill
Lower limit	.078	.28	72
Upper limit	.136	.38	62
Average	.107	.33	67

According to these estimates, if the resonance band is symmetrical about its maximum, the maximum should occur at $\tau_c = .107$ or at 67 percent fill-ratio. This implies a shift of maxima from τ_n

$$.107 - .112 = -.005$$

Such a displacement of maxima will remove the asymmetry. In our experiments, see Figure 8 for oil, the resonance curve is symmetrical.

The width of the band $\Delta\tau = .058$, whereas theoretical width $2\sqrt{S} = .017$. The ratio, therefore, is 3.3. Moreover, from Ward's graph of the rate of divergence of the nutational amplitude at resonance, the amplitude doubles in about 1.1 seconds. In our notation, this implies $\alpha_1 = 0.6$. The theoretical value is $\frac{\omega}{2}\sqrt{S} = 2.75$. The ratio, therefore, is 4.4.

These results were used in comparison with our experiments.